ENGINEERING RESEARCH INSTITUTE
UNIVERSITY OF MICHIGAN
ANN ARBOR

MAGNETIC MODULATION DESIGN

EMPLOYING MU SURFACES FOR FERRITES

Technical Report No. 37
Electronic Defense Group
Department of Electrical Engineering

By: L. W. Orr

Approved by: J. A. Boyd

Project 2262

TASK ORDER NO. EDG-4
CONTRACT NO. DA-36-039 sc-63203
SIGNAL CORPS, DEPARTMENT OF THE ARMY
DEPARTMENT OF ARMY PROJECT NO. 3-99-04-042
SIGNAL CORPS PROJECT NO. 194B
PLACED BY: SIGNAL CORPS ENGINEERING LABORATORY,
FORT MONMOUTH, NEW JERSEY

September, 1954

TABLE OF CONTENTS

LIST OF ILLUSTRATIONS

ABSTRACT

A practical design equation is derived for the transimpedance of a balanced magnetic modulator for small modulating current signals. Design is simplified by presenting incremental permeability as a three dimensional mu surface. Mu surfaces are shown for Ferramics G, H and I, and their application to magnetic modulator design is discussed.

MAGNETIC MODULATOR DESIGN EMPLOYING MU SURFACES FOR FERRITES

1. INTRODUCTION

Magnetic modulation of an rf carrier is very useful in a variety of applications. For example, it may be used in low level dc amplification, as in the measurement of very low current signals from low resistance thermocouples. In this instance it serves the same purpose as a high frequency chopper, but with several advantages over other chopper techniques. Balanced magnetic modulation may be used to eliminate the audio amplifier in the modulator of rf transmission systems, such as in telemetering and in single sideband systems where the carrier is absent.

A balanced magnetic modulator delivers an output voltage at the carrier frequency, the phase being determined by the polarity of the modulating signal, and the amplitude being proportional to the amplitude of the modulating signal. Since the input signal may be a varying dc current, the carrier may be at all times present. When an ac current signal is applied, the carrier is absent, and only sidebands are present. By proper core selection and circuit design, a magnetic modulator may be constructed with extremely small drift from the balance point. The presence of a dc unbalancing current in the input signal introduces a carrier voltage in the output for no ac signal. By adjusting the amount of unbalance, a normal modulation of any amount (up to 100% if desired) may be obtained for a given input signal level.

The input circuit of the modulator may be wound for a wide range of impedance levels to match the modulating source. When the input impedance is high a large inductance in the input circuit is generally implied; therefore, the upper limit of modulating frequencies may be restricted by circuit considerations.

The design equations derived for the simple magnetic modulator apply equally well to any magnetic material. However, the specific data given are for ferrites, or ferromagnetic spinels which are particularly well suited to high frequency operation. Carrier frequencies up to 50 mc or more may be used with ferrite cores, and satisfactory operation of a magnetic modulator at 10 mc carrier frequency has been obtained with little difficulty.

Modulating frequencies are generally limited to an order of magnitude lower than the carrier frequency. However, there may be additional limiting of the bandwidth of the modulating signal because of the inductance of the signal winding.

The input to a magnetic modulator is generally a current source, while the output is a modulated carrier voltage. In the balanced condition the ratio of output voltage (peak) to signal input current is called the transimpedance. An expression for the transimpedance of a simple magnetic modulator is derived.

It will be shown that mu surfaces are extremely useful in magnetic modulator design. In order to introduce the subject of mu surfaces, some basic properties of magnetic materials will first be considered.

2. INCREMENTAL PERMEABILITY

The basic physical property employed in magnetic modulation is the variation of incremental permeability μ_Δ with bias field H_o. Incremental permeability is defined as the ratio of Δ B to ΔH, when a toroidal specimen is cycled around a minor hysteresis loop such as 12341 in Fig. 1. ΔH is the range of excursion in applied magnetic field, while ΔB is the total excursion in flux density caused by the combined ac and dc fields. In Fig. 2 the dashed curve shows the position of the saturation B-H loop, or major hysteresis loop, for the material, and for any combination of ac and dc fields the specimen operates within this major loop. μ_Δ, the slope of the chord of a minor loop is generally smaller than the corresponding slope of the major loop at any particular value of B_o, but otherwise there is no particular relation between these slopes.

The manner in which the incremental permeability varies as a specimen of ferrite is cycled around a major B-H loop is demonstrated by the oscillogram, Fig. 2A. This shows a series of small excursions (minor loops) superposed on a major B-H loop for a toroid sample of Ferramic G[1]. This was obtained by a method in which the driving magnetic field applied to the sample contains two frequency components. The two frequencies used here were 60 cycles and 3000 cycles, so that the specimen performed 50 minor excursions for every excursion around the major loop.

To make the oscillogram clearer, half of the pattern (the negative-going portion of the major loop) was blanked off by a synchronized blanking pulse. The blanked protion would otherwise fall within the upper half of the major B-H loop (dashed line).

Since the audio amplifier used for driving the core was essentially a constant voltage generator, the size of ΔB for each small excursion was approximately constant over the range of H_o, while the size of ΔH varied because of the variation of μ_Δ.

[1] Ferramic G is a high frequency ferrite, Body No. 254, General Ceramics and Steatite Corporation, Keasbey, New Jersey.

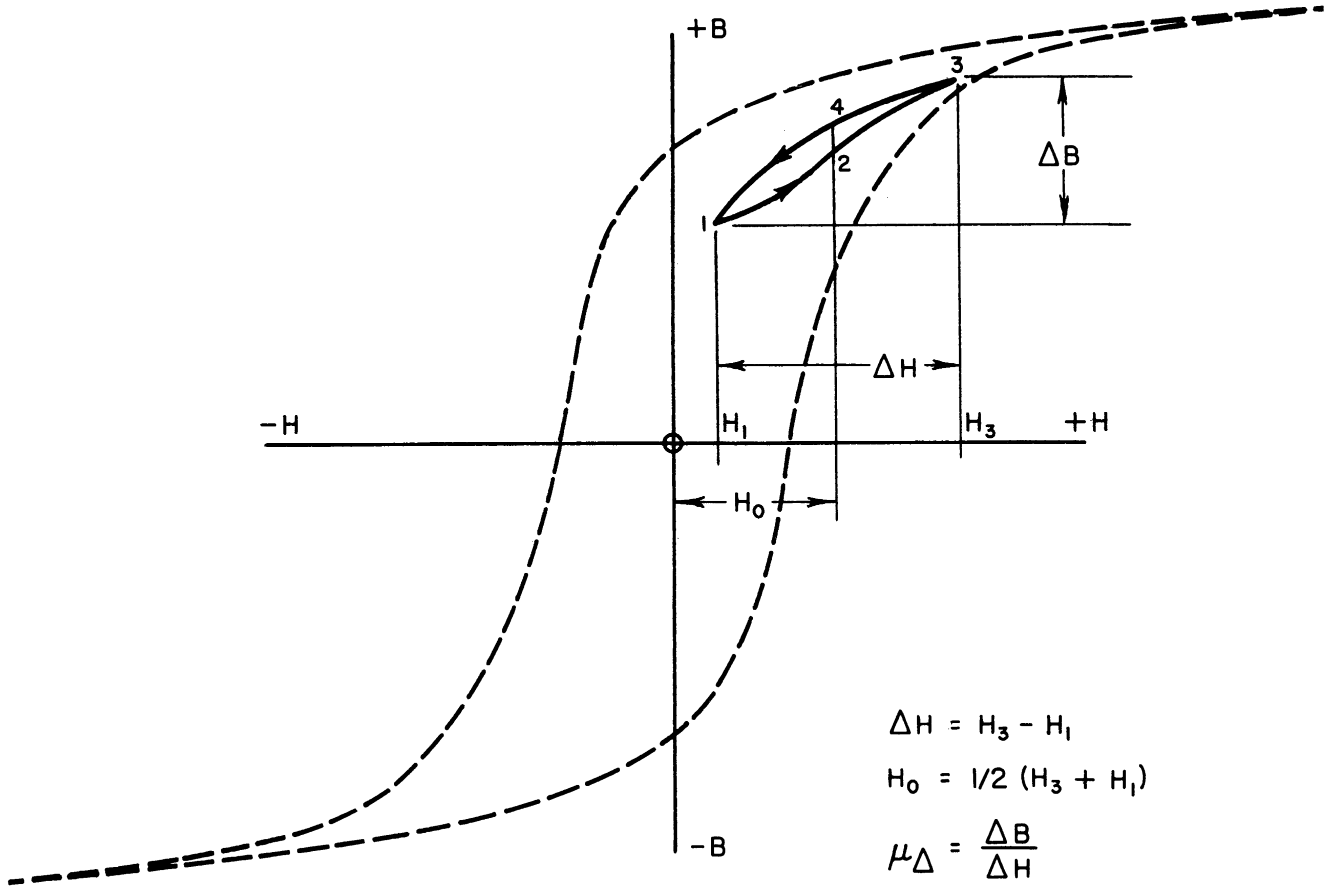

FIG. 1
DEFINITIONS OF MAGNETIC PARAMETERS

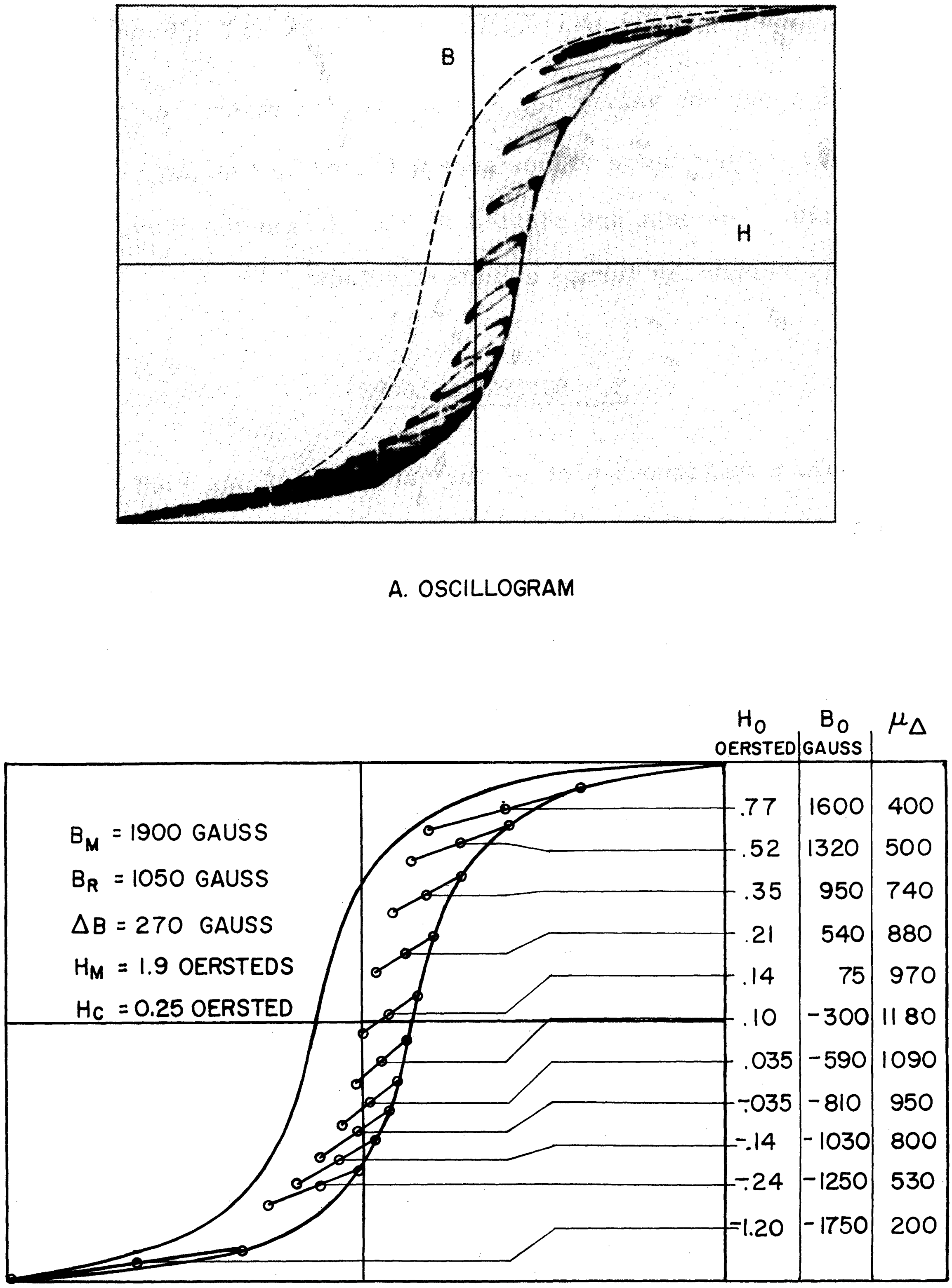

B. ANALYSIS OF A.

MULTIPLE HYSTERESIS LOOPS AT CONSTANT ΔB FOR FERRAMIC G

FIG. 2

Fig. 2B shows the values H_o, B_o and μ_Δ for several of the minor loops in the oscillogram. Since these values were obtained by scaling, the data are somewhat inaccurate. The data are plotted in Fig. 3, and the curve thus obtained is a μ_Δ-H curve, frequently termed a Butterfly Loop[1].

3. BUTTERFLY LOOPS

To obtain a continuous plot of the variation of μ_Δ with H_o, which gives greater accuracy than the previous method, the envelope of a radio frequency or high audio frequency wave, derived from the incremental flux excursions, is displayed as the abscissa with an ordinate proportional to H_o. A typical Butterfly Loop obtained in this manner[2] (in this case at constant ΔH) is shown in Fig. 4A. If the variations in H_o are confined to positive values only, a "half butterfly loop", or one-way μ_Δ-H loop, is generated, as shown in Fig. 4B.

4. μ_Δ -H LOOPS

As will be shown later, the mode of operation in magnetic modulation is such that the total magnetic field (the sum of the modulating signal, dc bias, and rf driving fields) does not change sign. For this reason, we will consider only the one-way μ_Δ-H loop. For semiquantitative work, the data may be obtained as in Fig. 4B. For more accurate work, the variations in μ_Δ must be found from

[1] The term Butterfly Loop is more usually applied to a plot of the variation of μ_Δ when ΔH is held constant.

[2] L. W. Orr, "Permeability Measurements in Magnetic Ferrites" EDG Technical Report No. 9, University of Michigan, September, 1952.

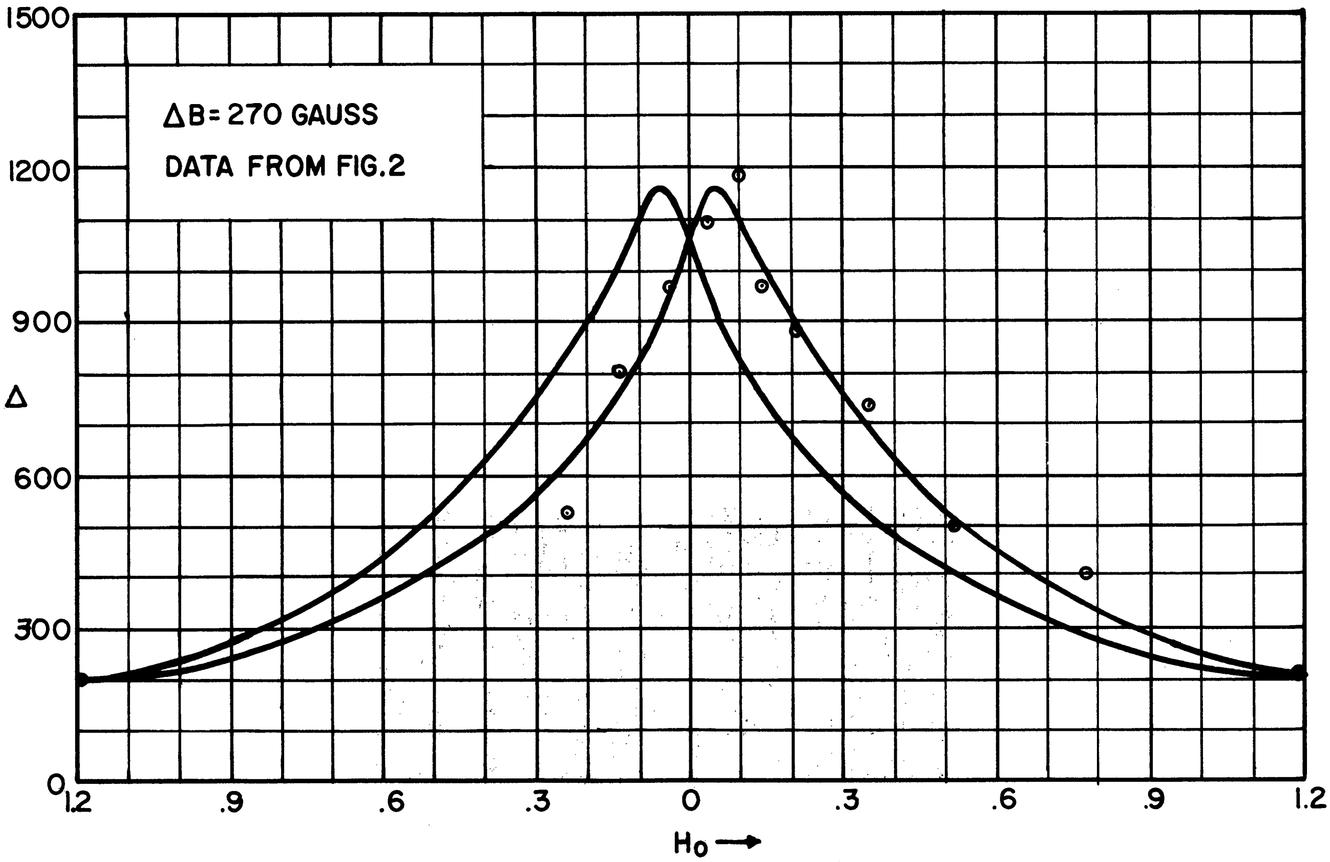

FIG. 3

BUTTERFLY LOOP AT CONSTANT ΔB FOR FERRAMIC G

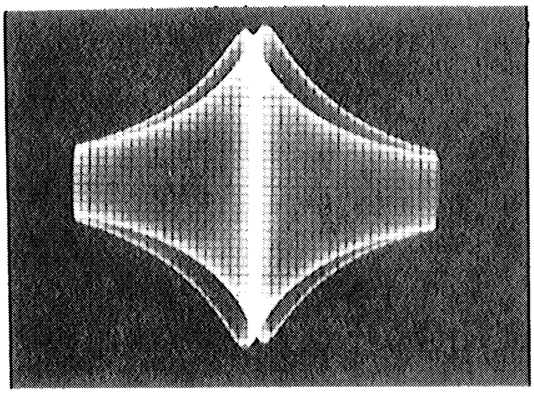

A. BUTTERFLY LOOP

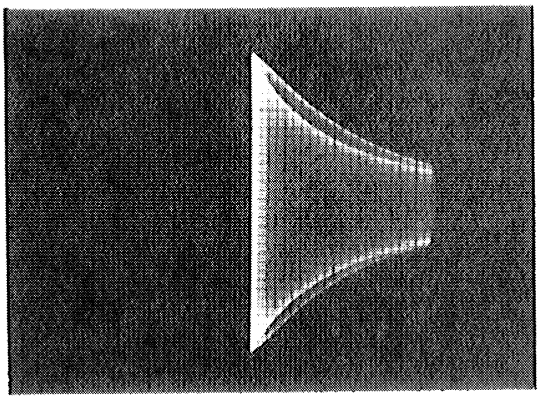

B. ONE-WAY μ-H LOOP

FIG. 4

μ-H OSCILLOGRAMS FOR FERRAMIC G

pointwise data using impedance measurements or a resonance method.

This variation of μ_Δ for a typical ferrite is shown by the one-way μ_Δ -H curves in Fig. 5. It is seen that each curve is double-valued, the higher value of permeability being obtained for H_o increasing. Curve B indicates less difference between the permeability for rising and falling H_o than does curve A. This serves to illustrate the fact that this discrepancy decreases as ΔH is increased. However, it is clear that there is also a variation in μ_Δ at constant H_o as ΔH is varied. In this case, the value of μ_Δ increases for curve B where ΔH is larger.

In many instances, such as in the design of a magnetic modulator, it is important to examine the manner in which μ_Δ varies when both H_o and ΔH are variable. A display of such data may be accomplished by plotting a family of curves, such as A and B in Fig. 5, but a much clearer presentation is a three-dimension plot, or mu surface.

5. MU SURFACES

By plotting μ_Δ as a function of both H_o and ΔH in three dimensions, a mu surface[1] is obtained. Isometric projections of three mu surfaces are shown in Figs. 6, 7 and 8. These surfaces were obtained from Type F109 toroid samples of Ferramic bodies G-254, H-419 and I-141. The permeability was measured at 25° C using a frequency of 10 kc. Each surface was obtained by taking a series of oscillograms similar to Fig. 4B. From these the surface contours were plotted in isometric projection. The curve for $\Delta H = 0$ (dotted line, Figs. 5, 6 and 7) was obtained by **extrapolating** the curves of constant H_o back to the plane $\Delta H = 0$. The

1 L. W. Orr, "Permeability Measurements in Magnetic Ferrites" EDG Technical Report No. 9, University of Michigan, September, 1952.

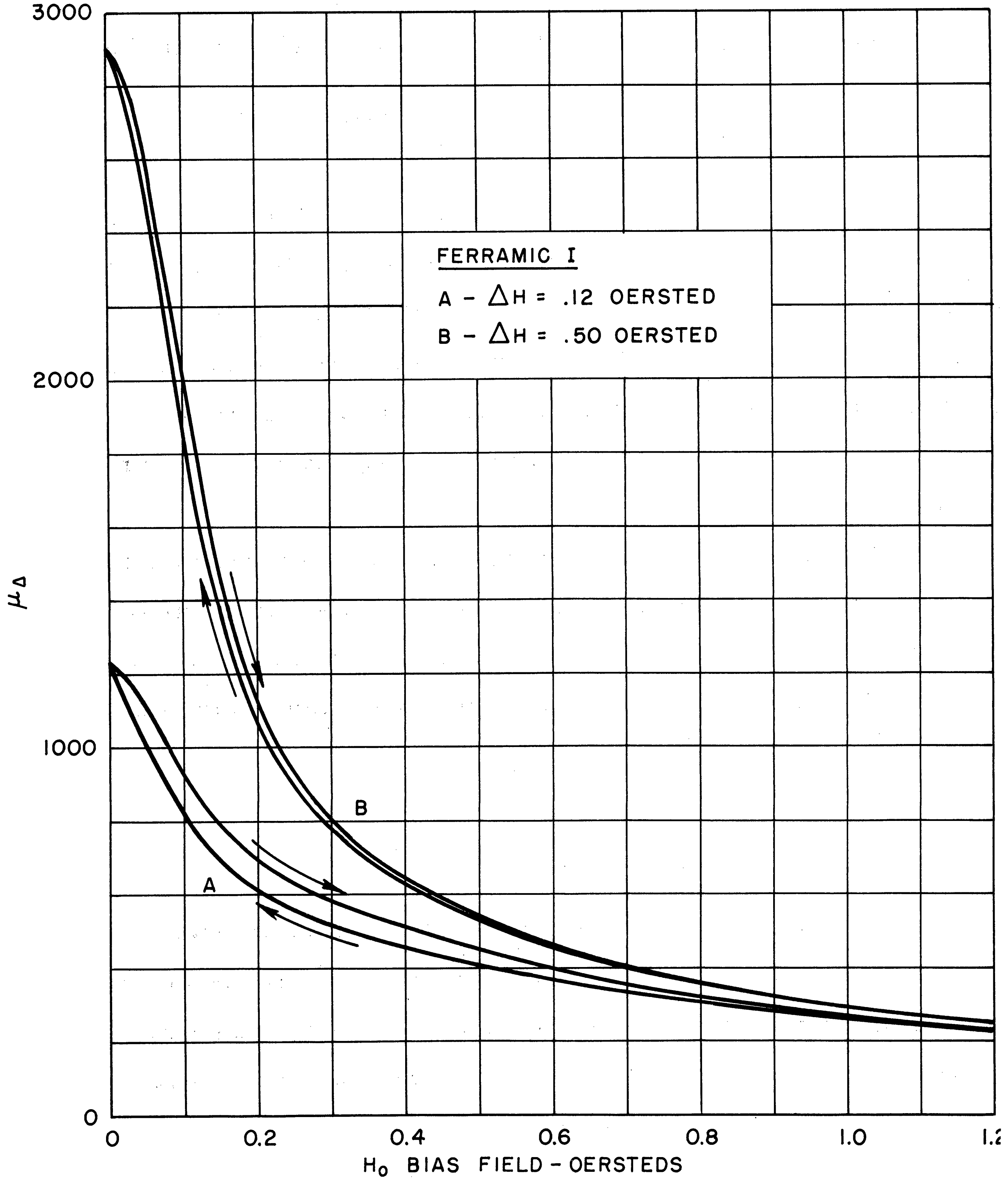

FIG. 5

VARIATION OF INCREMENTAL PERMEABILITY WITH BIAS FIELD IN FERRAMIC I.

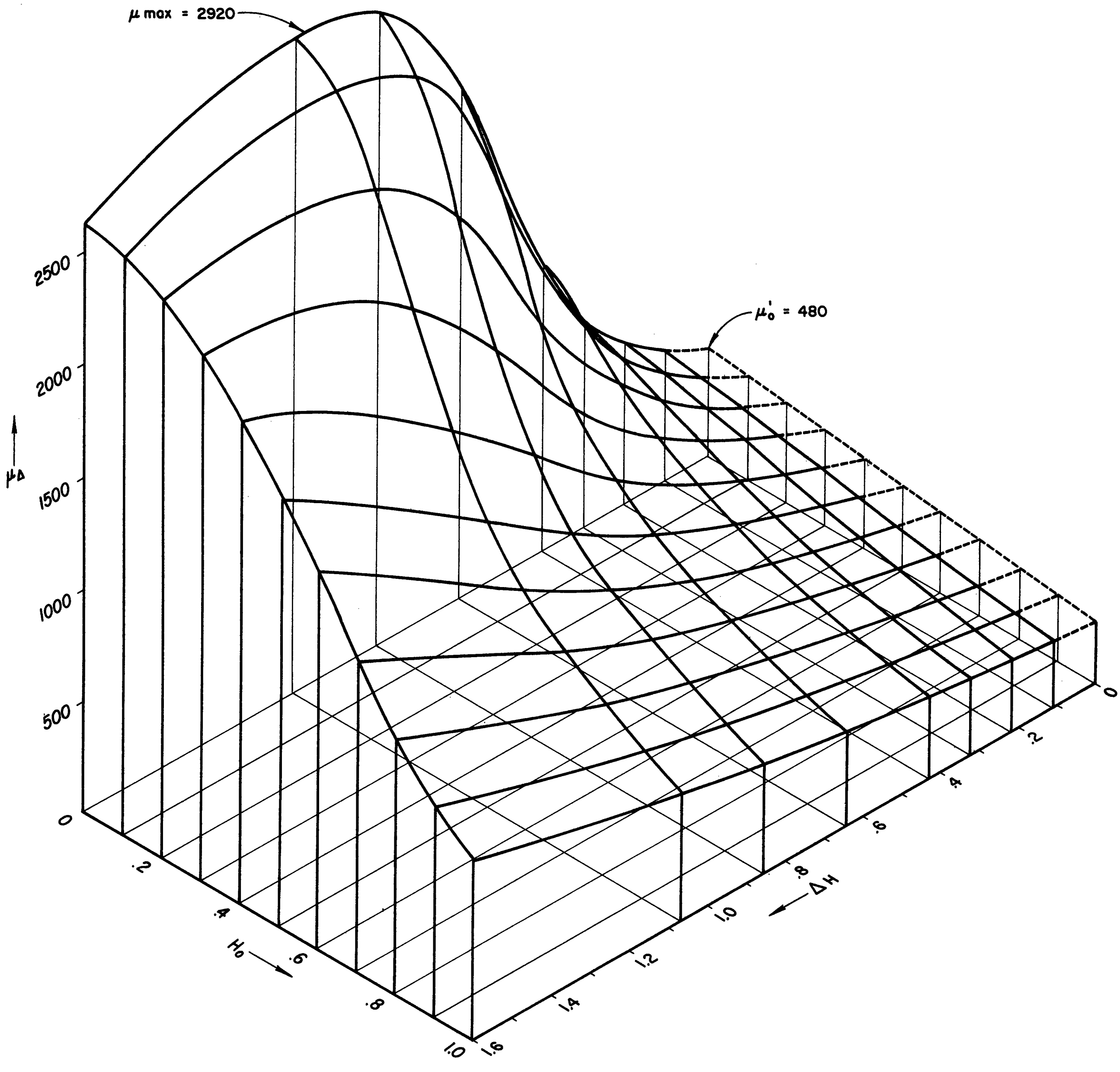

FIG. 6
MU SURFACE FOR FERRAMIC G

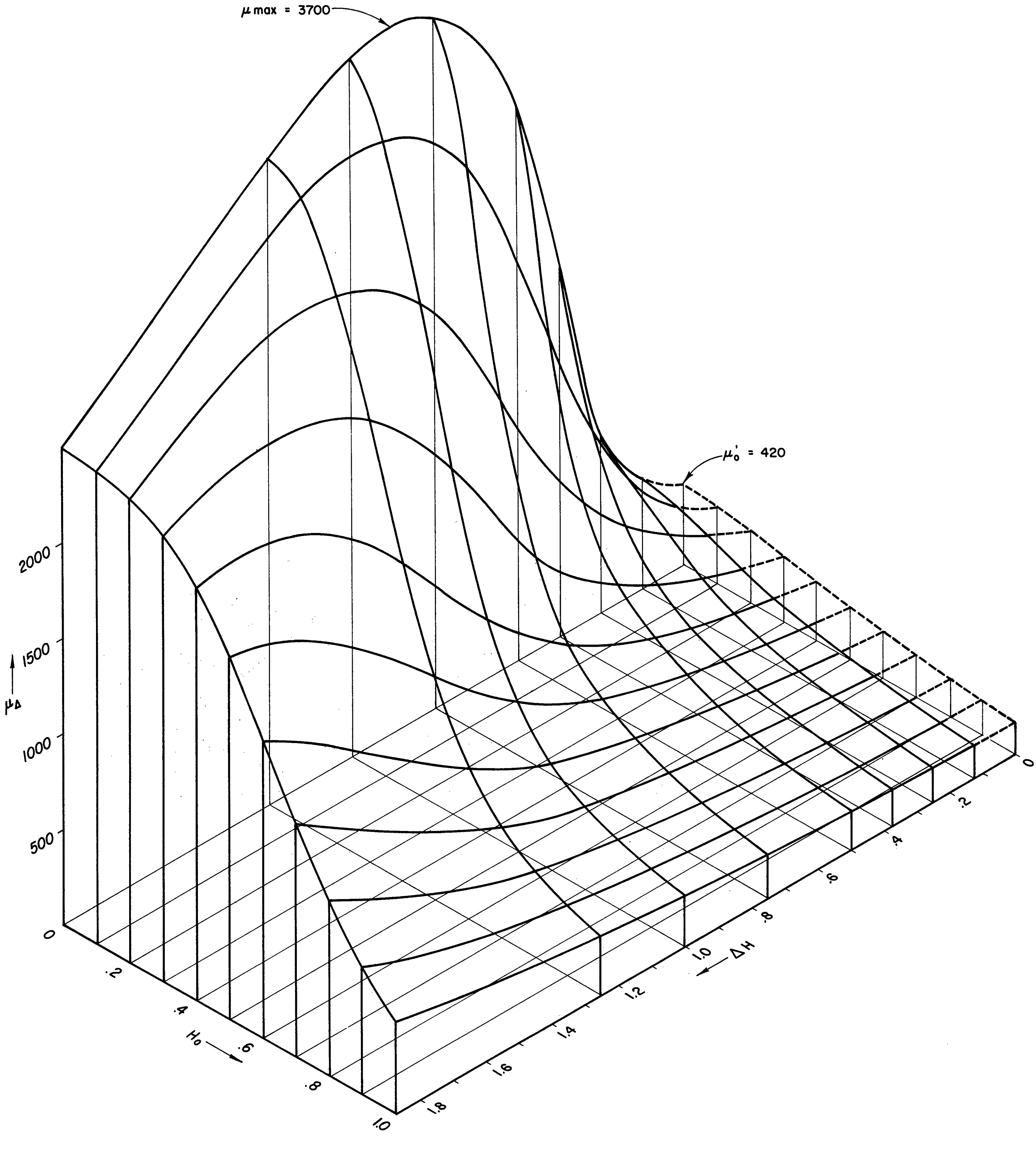

FIG. 7
MU SURFACE FOR FERRAMIC H.

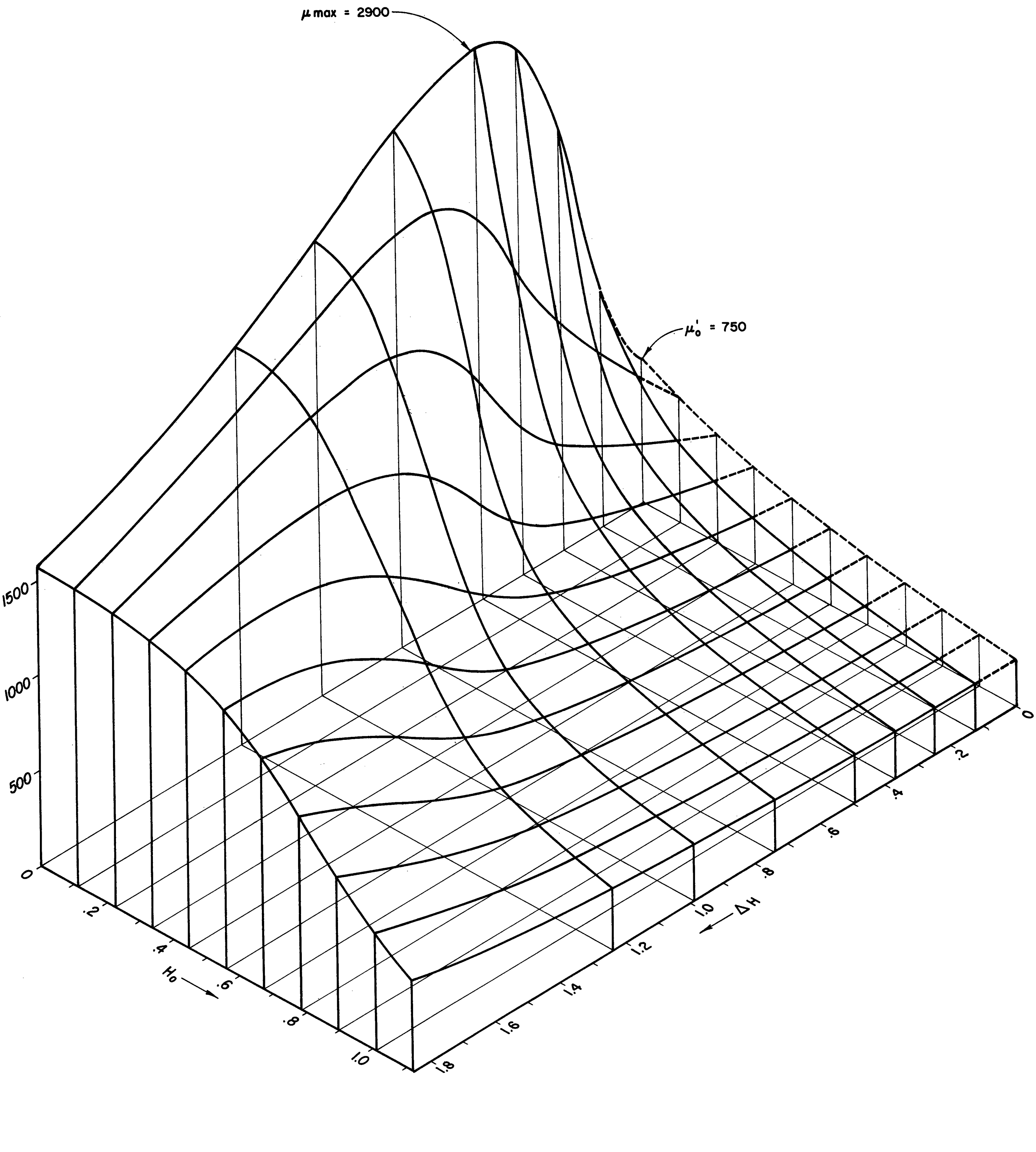

FIG. 8
MU SURFACE FOR FERRAMIC I

intercept of this $\Delta H = 0$ curve at the origin is the value μ_o' to distinguish it from the true initial permeability, μ_o. The values of μ_o' and μ_{max} are given in each figure.

Since it is seen in Fig. 5 that each μ_Δ -H_o curve is double valued, the mu surface is really a double surface. The upper branch of this surface is for H_o increasing, while the lower branch is for H_o decreasing. To avoid confusion, only the upper mu surface is plotted in Figs. 6, 7 and 8. The spacing between the two branches of the surface becomes quite small for large values of H_o and ΔH, the trend being indicated in curve B of Fig. 5. In most regions of the surface, the slope $d\mu_\Delta/dH_o$ is very nearly the same for the upper and lower branches. This is an important point, since the derivative is the important factor in modulator design.

Mu surfaces for various magnetic ferrites make it possible to solve readily several types of magnetic design problems, and to answer such questions as the following. What is the best material for the job? What is the operating point for the maximum sensitivity? What is the operating point for the minimum distortion at a specified signal level?

The application of mu surfaces in magnetic modulator design will be discussed in detail in the next section.

6. MAGNETIC MODULATOR DESIGN

6.1 Simple Balanced Modulator

One of the simplest forms of balanced magnetic modulators is shown in Fig. 9. It consists of two similar ferrite toroid cores (a and b, Fig. 9) of uniform rectangular cross section. These are wound with excitation windings 1(a) and 1(b) of N_1 turns each and connected in series. These windings are excited by

M-970 A-S4-38 JEM 5-21-53

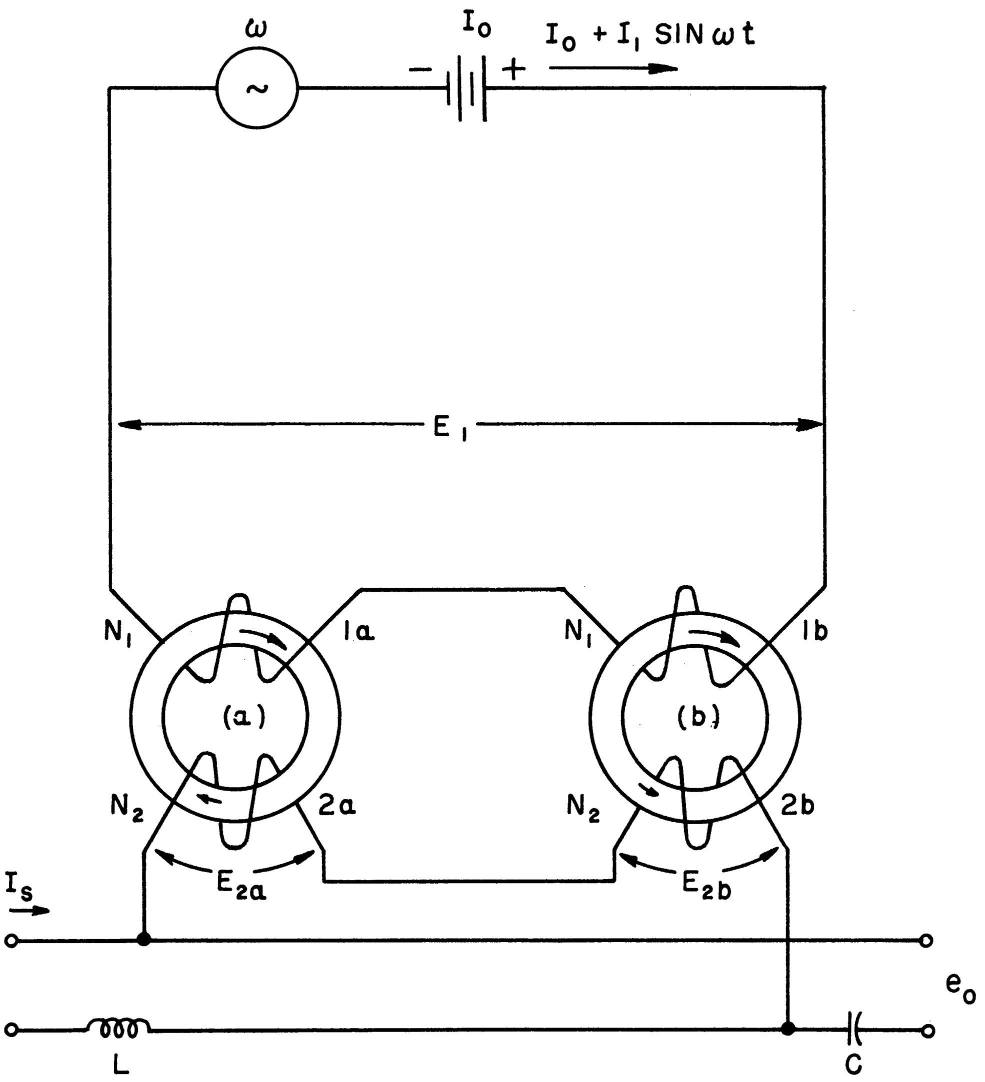

FIG. 9

SIMPLE BALANCED MAGNETIC MODULATOR.

rf and dc current generators giving a combined current of $I_1 \sin \omega t + I_o$ amperes. A dc signal current, I_s, is fed through isolating inductor L, to the secondary windings 2(a) and 2(b) connected in series opposition, and when properly balanced, the output voltage e_o is an rf carrier having its magnitude and phase related respectively to the size and polarity of the signal current I_s.

The operating characteristic of each core is shown in Fig. 10. When $I_s = 0$, both cores operate at the point P by virtue of the dc bias current I_o, and there is zero output voltage. When a positive signal current flows, core "a" is made to operate at point A while core "b" is made to operate at point B (see Fig. 10). An expression for the peak amplitude E_o of the fundamental component of the output wave may be obtained by assuming a sinusoidal variation of flux density in the two cores. The resulting expression[1] is

$$E_o = \frac{N_2 A\omega(\mu b - \mu a) N_1 I_1 10^{-8}}{5r} \text{ volts peak.} \qquad (1)$$

Where N_1 and N_2 are the number of primary and secondary turns on each core, A is the cross section area in square centimeters of each core, ω is the angular frequency of exciting current of amplitude I_1, μ_a and μ_b are the incremental permeabilities at points A and B in Fig. 10, and r is the mean magnetic radius[2] in centimeters of the toroids.

---

[1] This expression is derived in Appendix A.

[2] The mean magnetic radius r of a toroid of uniform rectangular cross section and inner and outer radii r_1 and r_2 is given by

$$r = \frac{r_2 - r_1}{\log_e r_2 - \log_e r_1} .$$

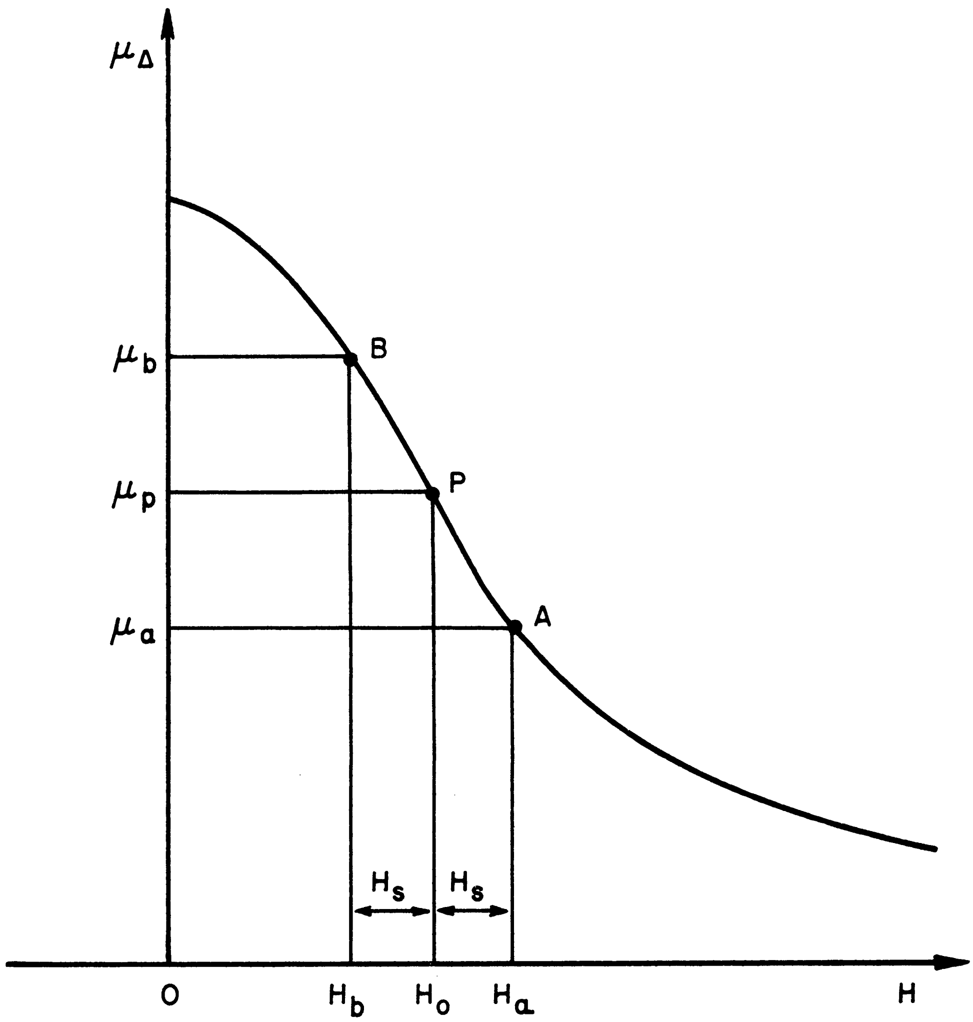

FIG. 10

OPERATING CHARACTERISTIC OF MODULATOR.

6.2 Calculation of Transimpedance

Over a small range in H, in which the operating characteristic may be considered linear, we may write

$$(\mu_b - \mu_a) = 2H_s \left(\frac{d\mu\Delta}{d H_o}\right)_P \qquad (2)$$

where the derivative is taken at the point P, and H_s is the small additional field derived from the signal current I_s as in Fig. 10. Noting also that

$$H_s = \frac{N_2 I_s}{5r} \qquad (3)$$

we may substitute (2) and (3) in (1) to obtain

$$E_o = \frac{2 A\omega N_1 I_1 N_2^2 I_s}{25 r^2} \left(\frac{d\mu\Delta}{d H_o}\right)_p 10^{-8} \text{ volts} \qquad (4)$$

In most applications, the input exciting voltage E_1 is restricted to practical limits by oscillator design considerations. It is convenient to introduce a design peak value of E_1 such that

$$E_1 = E_{1a} + E_{2a}$$

$$= 2\omega L_1 I_1 \text{ volts peak.}$$

where $$L_1 = \frac{\mu_{\Delta p} A N_1^2}{5r} 10^{-8} \text{ hen., for } I_s = 0.$$

So $$E_1 = \frac{2\omega \mu_{\Delta p} A N_1^2 I_1}{5r} 10^{-8} \text{ volts peak.} \qquad (5)$$

By substitution in Eq. 4, we have

$$E_o = \frac{E_1}{5r N_1 \mu_{\Delta p}} N_2^2 I_s \left(\frac{d\mu\Delta}{d H_o}\right)_p \text{ volts peak.} \qquad (6)$$

where $\mu_{\Delta p}$ and $\left(\frac{d\mu_\Delta}{dH_o}\right)_p$ are the values of incremental permeability and its derivative taken at the operating point P. The transimpedance, Z_t, of the device is the ratio of change in peak output voltage E_o to a change in signal current I_s. Thus,

$$Z_t = \frac{E_o}{I_s} = \frac{E_1}{5r\, N_1\, \mu_{\Delta p}} \quad N_2^2 \left(\frac{d\mu_\Delta}{dH_o}\right)_p \qquad (7)$$

This equation illustrates the following factors in modulator design:

1. The transimpedance increases with E_1.
2. The transimpedance decreases as $\mu_{\Delta p}$ increases. This is caused by the fact that the inductive reactance of the driving windings increases with $\mu_{\Delta p}$ thus reducing the exciting current I_1.
3. The transimpedance increases with N_2^2. Since the inductance L_2 of the output windings also increases with N_2^2, E_o will vary directly with L_2.
4. The transimpedance varies with the derivative $(d\mu_\Delta/dH_o)$. This is one of the critical variables and must be selected by a proper choice of magnetic material and operating conditions. For the maximum sensitivity (highest transimpedance), this derivative must be as large as possible. On the other hand, if minimum distortion is required, the operating point should be chosen for little or no variation in $(d\mu_\Delta/dH_o)$ over the desired range of operation.

The next section shows how mu surfaces may be used to facilitate the selection of a suitable material and operating point with regard to $(d\mu_\Delta / dH_o)$.

5. The transimpedance is unaffected by varying the frequency. This follows since ω is absent from Eq. 6. It is often believed that a higher transimpedance is obtained by operating at a higher carrier frequency, and Eq. 4 would lead to this conclusion. However, it should be pointed out that as the frequency is raised, the inductive reactance L_1 of the driving windings increases. This causes a reduction in the driving current I_1 with the result that the product ωI_1 in Eq. 4 remains constant as ω is varied. Therefore, the transimpedance is invariant with frequency.

6.3 Other Design Features

Although the transimpedance is generally the most important factor in modulator design, several other factors must be considered. For example, the core material must be chosen to have a relatively low total loss at the carrier frequency, otherwise additional driving power and overheating of the cores may become a problem.

In addition, the turns on the signal winding, N_2, may not always be made as large as desired because of excessive inductance in the input circuit. The choice of N_2 and of the isolating inductance L, thus depend to a large extent upon the bandwidth of the modulating signal to be used. A further restriction on N_2 may come from the output circuit, where particular requirements are needed. If the output is to drive a vacuum tube, it must work into the capacitive input of the tube. It may be occasionally desirable to resonate the output inductance with this capacitance to obtain the argest possible output voltage. In general this is avoided however, so that a ritical adjustment is not required, and so that small fluctuations in output inductance, driving frequency, or stray capacitance do not affect the operation of the modulator.

Certain assumptions were made in deriving the transimpedance which may not be precisely true. For example, it was assumed that the incremental permeability was a single valued function of H_o although it is shown in Fig. 5 to be double valued. A first consequence of this is that the application and removal of a rather large pulse of signal current to a balanced modulator will slightly upset the balance giving a small amount of carrier for no signal. A second consequence is that there will generally be a small phase shift between the input current waveform and the envelope of the modulator output. However, these effects are generally small enough to be ignored.

It was also assumed that the rf excitation current was sinusoidal. However, slight variations of the total impedance of the driving windings, and the nonlinearity of the core material may cause the excitation current to be modulated by the signal current, and to contain harmonics of the carrier frequency. It may be necessary in some applications to remove the harmonic content[1] of the modulator output by means of a low-pass filter.

6.4 Application of Mu Surfaces

As noted above, the derivative ($d\mu_\Delta / dH_o$) is the important factor in modulator design. A proper choice of magnetic material and operating conditions may be directly obtained from mu surfaces.

For maximum small signal transimpedance, the material having the largest derivative is selected. By examining Figs. 6, 7 and 8 it is found that Ferramic I

---

[1] In another type of magnetic modulator called a magnettor, the carrier is filtered out and only the second harmonic is used as the modulator output. This is described in Article 8 of the Bibliography.

will give the greatest Z_t. Although this material has a maximum permeability (μ_{max} = 2900) smaller than others, such as Ferramic H, its maximum derivative $\left[(d\mu_\Delta/dH_o)_{max} = 12,700 \text{ per oersted}\right]$ is largest.

The point on the mu surface where $(d\mu_\Delta/dH_o)_{max}$ is found also gives the correct operating point for each core of the modulator. In this case the cores should operate at H_o = 0.05 oe., and ΔH = 0.37 oe.

6.5 Practical Design of a High-Z_t Modulator

As an example of the method of using the design equations and mu surfaces, the design values for a typical high sensitivity modulator are given. It is assumed that the F-109 core size is satisfactory, and this determines the values of r and A. Ferramic I is chosen as the best material of the three for which mu surfaces are shown in this report. This determines the values of $(d\mu_\Delta/dH_o)_{max}$ and $\mu_{\Delta p}$, found from the mu surface as described above, and fixes the operating point at H_o = 0.05 oe, and ΔH = 0.37 oe., which determines the size of I_o and I_1 once the excitation windings (N_1) are designed.

In the design given, N_1 was chosen as 50 turns, and N_2 was chosen as 200 turns. The choice of N_1 is not arbitrary, but is chosen to work with a particular driving frequency. In this case, however, we shall choose N_1 arbitrarily, and calculate the required driving frequency. It is assumed that rf power is available at 100 volts peak.

These design values are tabulated as follows:

r = 0.9 cm	$\left(\dfrac{d\mu_\Delta}{dH}\right)_p = 12.7 \times 10^3$
A = 0.1 cm^2	
N_1 = 50 turns	$\mu_{\Delta p} = 2 \times 10^3$
N_2 = 200 turns	H_o = 0.05 Oe
E_1 = 100 v. peak	ΔH = 0.37 Oe

To satisfy the operating point conditions, the required values of I_o and I_1 are found.

$$I_o = 5rH_o/N_1 = 4.5 \text{ ma.}$$

$$I_1 = 5r(1/2\Delta H)/N_1 = 16.2 \text{ ma. (peak)}$$

Since we do not have arbitrary control of the current I_1, the frequency must be adjusted so that the proper value of I_1 will flow. By rearranging Eq. 5 for frequency determination, we have

$$f = \frac{\omega}{2\pi} = \frac{5 \times 10^8 E_1 r}{4\pi I_1 \mu_{\Delta_p} A N_1} = 444 \text{ kc.}$$

Finally, the transimpedance is found from Eq. 7, and has the value

$$Z_t = 0.112 \times 10^6 \text{ volts per ampere.}$$

7. CONCLUSIONS

The design of magnetic modulators is greatly simplified by the use of mu surfaces. Although the derivation $\frac{du_o}{dH_o}$ is of primary importance in modulator design, it was noted that other factors must be considered.

Although not described in detail in this report, the mu surface may be applied to the design of many types of magnetic modulators and other magnetic devices (e.g., magnetic tuning of rf circuits) whose operation depends on the variation of incremental permeability.

APPENDIX A

Derivation of expression for peak amplitude E_o of fundamental component of output voltage. (Eq. 1).

Assumptions

1. The r-f flux varies sinusoidally in both cores.
2. The operating characteristic (Fig. 10) is single-valued.
3. The isolating inductance L produces no loading upon the output.

According to assumption 1, the flux density $B = B_1 \sin \omega t$ so that

$$\frac{dB}{dt} = \omega B_1 \cos \omega t$$

In each core, the voltage e_2 in the secondary is

$$e_2 = N_2 \frac{d\phi}{dt} \quad 10^{-8} \quad \text{volts}$$

$$= N_2 A \omega B_1 \cos \omega t \quad 10^{-8} \quad \text{volts}$$

$$= N_2 A \omega \mu_\Delta H_1 \cos \omega t \quad 10^{-8} \quad \text{volts}$$

But $H_1 = \frac{N_1 I_1}{5r}$ Oe.

Thus, the peak value of voltage across winding 2a is

$$E_{2a} = \frac{N_2 A\omega \mu_a N_1 I_1 10^{-8}}{5r} \quad \text{volts}$$

A similar expression may be written for E_{2b}. These two voltages are 180° out of phase so that the peak output voltage E_o is their difference, thus

$$E_o = \frac{N_2 A\omega (\mu_a - \mu_b) N_1 I_1}{5r} \quad 10^{-8} \quad \text{volts.}$$

Bibliography

1. E. Peterson, J. M. Manley, and L. R. Wrathall, "Magnetic Generation of a Group of Harmonics." B.S.T.J., 16, 437, October 1937.

2. A. S. Fitzgerald, "Magnetic Amplifier Circuits." Jour. Franklin Inst., 244, p. 249, October 1947.

3. A. U. Lamm, "Some Fundamentals of a Theory of the Transductor or Magnetic Amplifier." Trans. AIEE, 66, p. 1078, 1947.

4. L. W. Buechler, "Magnetic Amplifiers for Shipboard Applications." Elec. Engr., 68, p. 33, January 1949.

5. R. E. Morgan, "The Amplistat--A Magnetic Amplifier." Elec. Engr., 68, p. 663, August 1949.

6. Gunnar Wennerberg, "A Simple Magnetic Modulator for Conversion of Millivolt D-C Signals." Elec. Engr., 70, p. 144, February 1941.

7. J. M. Manley, "Some General Properties of Magnetic Amplifiers." Proc. IRE, 39, p. 242, March 1951.

8. E. P. Felch, V. E. Legg and F. G. Merrill, "Magnetic Modulators." Electronics, 25, p. 113, February 1952.

DISTRIBUTION LIST

1 copy	Director, Electronic Research Laboratory Stanford University Stanford, California Attn: Dean Fred Terman
1 copy	Chief, Electronic Warfare Department Army Electronic Proving Ground Fort Huachuca, Arizona
1 copy	Chief, Engineering and Technical Division Office of the Chief Signal Officer Department of the Army Washington 25, D. C. Attn: SIGJM
1 copy	Chief, Plans and Operations Division Office of the Chief Signal Officer Washington 25, D. C. Attn: SIGOP-5
1 copy	Countermeasures Laboratory Gilfillan Brothers, Inc. 1815 Venice Blvd. Los Angeles 6, California
1 copy	Commanding Officer White Sands Signal Corps Agency White Sands Proving Ground Las Cruces, New Mexico Attn: SIGWS-CM
1 copy	Commanding Officer Signal Corps Electronics Research Unit 9560th TSU Mountain View, California
75 copies	Transportation Officer, SCEL Evans Signal Laboratory Building No. 42, Belmar, New Jersey FOR - SCEL Accountable Officer Inspect at Destination File No. 22824-PH-54-91(1701)

1 copy	H. W. Welch, Jr. Engineering Research Institute University of Michigan Ann Arbor, Michigan
1 copy	Document Room Willow Run Research Center University of Michigan Willow Run, Michigan
11 copies	Electronic Defense Group Project File University of Michigan Ann Arbor, Michigan
1 copy	Engineering Research Institute Project File University of Michigan Ann Arbor, Michigan

EDG - TECHNICAL REPORT NO. 37

ERRATA

Page 3 line 4 -- Fig. 2 - should be Fig. 1.

Page 23, Section 7 line 2

$$\frac{du_o}{dH_o} \quad \text{should be} \quad \frac{d\mu_\Delta}{dH_o}$$